

Phase diagrams and superconductivity of ternary Ca-Al-H compounds under high pressure

Ming Xu¹, Defang Duan², Wendi Zhao¹, Decheng An², Hao Song^{1,*} and Tian Cui^{1,2,†}

¹*Institute of High Pressure Physics, School of Physical Science and Technology, Ningbo University, Ningbo 315211, China*

²*State Key Laboratory of Superhard Materials, College of Physics, Jilin University, Changchun 130012, China*

*Corresponding author: songhao@nbu.edu.cn

†Corresponding author: cuitian@nbu.edu.cn

Abstract

The search for high-temperature superconductors in hydrides under high pressure has always been a research hotspot. Hydrogen-based superconductors offer an avenue to achieve the long-sought goal of superconductivity at room temperature. We systematically explore the high-pressure phase diagram, electronic properties, lattice dynamics and superconductivity of the ternary Ca-Al-H system using *ab initio* methods. We found two stable ternary hydrides at 50 GPa: *Cmcm*-CaAlH₅ and *Pnmm*-CaAl₂H₈, which both are semiconductors. At 200 GPa, a new phase of *P2₁/m*-CaAlH₅, *P4/mmm*-CaAlH₇ and a metastable compound *Immm*-Ca₂AlH₁₂ were found. Furthermore, *P4/mmm*-CaAlH₇ has obvious phonon softening of high frequency vibrations along the Z-A direction, point A and point X, which improves the strength of electron-phonon coupling. Therefore, a superconducting transition temperature T_c of 71 K is generated at 50 GPa. In addition, the thermodynamic metastable *Immm*-Ca₂AlH₁₂ exhibits a superconducting transition temperature of 118 K at 250 GPa. These results are very useful for the experimental searching of new high- T_c superconductors in ternary hydrides.

I. INTRODUCTION

The researches on superconducting properties of materials have always been one of the hotspots in condensed matter physics, and the room temperature superconductivity has always been the long-sought goal pursued by most researchers. Since hydrogen is the lightest element in nature and exhibit substantially high Debye temperature^[1], metallic hydrogen has been expected to be a candidate for room-temperature superconductor and synthesize under high pressure^[2], so researchers have set off an upsurge in the investigation for metallic hydrogen for a long time. The metallization of hydrogen requires extremely high-pressure conditions^[3-5], which is difficult to achieve. The experimental observation of metallic hydrogen is still controversial. But at the beginning of this century, Aschroft came up with a great pioneering idea^[6], "chemical precompression", which means that hydrogen-rich materials probably can be metallized at lower pressures and exhibit high temperature superconductivity. So far, the most of binary hydrides have been explored theoretically, and many excellent results have been obtained^[7-10]. The superconducting transition temperature T_c exceeds 200 K in binary hydrides at high pressure, such as HfH₁₀ with T_c of 234 K at 250 GPa^[11], YH₆ with T_c of 264 K at 120 GPa^[12], YH₁₀ with T_c of 303 K at 400 GPa^[13], ThH₁₀ with T_c of 241 K at 100 GPa^[14], CaH₆ with T_c of 235 K at 150 GPa^[15].

Especially the theoretical and experimental results of LaH_{10} ^[16-19] and H_3S ^[20-23] have great significance in the field of high temperature superconductivity. H_3S exhibits a high T_c of 203 K and adopting a covalent sixfold cubic structure. The hydrogen-rich compound LaH_{10} has H_{32} cage with a sodalite-like structure, showing a high T_c of 250 K at 170 GPa. The common features^[7] of these high-temperature hydrogen-rich superconductors are relatively high symmetry, high density of states at the Fermi level and strong electron-phonon coupling.

As the binary hydrides have been widely studied, the researches on ternary hydrides have gradually begun. Comparing with binary hydrides, ternary hydrides offer more abundant structures caused by the diversity of chemical compositions. Hydrogen-rich ternary compounds may undergo metallization at lower pressures due to the "chemical precompression" from the third element. Moreover, the hydrogen-rich compounds are more likely to exhibit high density of states at the Fermi level, which makes them strong contenders for high-temperature superconductors. Recently, the theoretical prediction on the ternary hydrides have also achieved good results^[24-28]. For example, $\text{Li}_2\text{MgH}_{16}$ exhibits an unprecedentedly high T_c of 473 K at 250 GPa^[27]. Ternary compounds formed by introducing lithium into the yttrium hydrides under pressure, especially LiYH_9 with a T_c of 109 K at 250 GPa^[25]. Through theoretical calculations, CaBH_7 has a T_c of 135 K at 150 GPa^[24,28], and NaAlH_8 exhibits phonon anomalies which caused by Fermi surface nesting with a T_c of 55 K at 300 GPa^[26].

In this paper, we report a first-principles study results of the Ca-Al-H system. The $Pnmm$ - CaAl_2H_8 and $Cmcm$ - CaAlH_5 are semiconductors at 50 GPa. $P4/mmm$ - CaAlH_7 is thermodynamic stable at 200 GPa, while the $Immm$ - $\text{Ca}_2\text{AlH}_{12}$ is metastable. CaAlH_7 and $\text{Ca}_2\text{AlH}_{12}$ are good metals which both containing H and H_2 units, with superconducting transition temperatures of 71 K at 50 GPa and 118 K at 250 GPa, respectively. We proposed five possible synthetic routes ($\text{Ca}+\text{Al}+\text{H}_2$, $\text{Ca}+\text{AlH}_3+\text{H}_2$, $\text{CaH}_2+\text{Al}+\text{H}_2$, $\text{CaH}_2+\text{AlH}_3+\text{H}_2$, $\text{CaH}_4+\text{Al}+\text{H}_2$) and demonstrate their enthalpies of formation for the Ca-Al-H compounds, which will contribute to subsequent experimental studies. Our work has important implications for understanding the high-pressure phase diagram and fundamental properties of the Ca-Al-H ternary system.

II. COMPUTATIONAL DETAILS

We performed variable composition structure searches using *ab initio* random structure searching code (AIRSS)^[29,30]. For $\text{Ca}_x\text{Al}_y\text{H}_z$ ($1 \leq x \leq 2$, $1 \leq y \leq 2$, $1 \leq z \leq 12$) at 50 and 200 GPa over 10,000 structures were predicted. The Cambridge Series Total Energy Package (CASTEP)^[31-33] software was used to determine the stable structure on the ternary phase diagram. The cut-off energy of the plane wave was set to 300 eV, and the sampling grid spacing of the selected Brillouin zone was $2\pi \times 0.07 \text{ \AA}^{-1}$. the candidates and previously reported structures underwent high-quality parameter re-optimization. To precisely converge the enthalpy calculation to less than 1 meV/atom, the Brillouin zone k -point mesh was sampled with $2\pi \times 0.03 \text{ \AA}^{-1}$, and the cut-off energy was set to be 800 eV.

Calculations of electronic properties were performed using the Vienna *ab initio* Simulation Package (VASP)^[34], the projected augmented wave method (PAW)^[35] was used to simulate the interaction between electrons and ions. $3s^23p^64s^2$, $3s^23p^1$ and $1s^1$ were considered as valence electrons for Ca, Al and H, respectively. We used a generalized gradient approximation (GGA) with the Perdew-Burke-Ernzerhof (PBE) parametrization for the exchange-correlation

functional^[36]. The cut-off energy was set to 800 eV and the Monkhorst-Pack k mesh $2\pi \times 0.03 \text{ \AA}^{-1}$ was used, a denser k mesh $2\pi \times 0.01 \text{ \AA}^{-1}$ was used to obtain high precise results of electronic properties. Phonon spectra and electron-phonon coupling were calculated using the Quantum-Espresso package^[37]. The ultrasoft pseudopotential (USPP) and the plane wave cut-off energy of 80 Ry were used. For $P4/mmm$ - CaAlH_7 $24 \times 24 \times 16$ k mesh and $6 \times 6 \times 4$ q mesh were used, for $Immm$ - $\text{Ca}_2\text{AlH}_{12}$ $16 \times 16 \times 16$ k mesh and $4 \times 4 \times 4$ q mesh were used. Considering that the EPC parameters λ of the all hydrides we investigated are less than 1.5, the Allen-Dynes modified McMillan equation^[38] is selected to estimate the superconducting transition temperature T_c .

III. RESULTS AND DISCUSSION

A. Ternary phase diagrams and different synthetic routes of ternary hydrides

Ca-H and Al-H binary compounds have been systematically studied, and some binary compounds exhibit superconducting properties under high pressure^[15,39,40]. Here, we performed structure searches for $\text{Ca}_x\text{Al}_y\text{H}_z$ ($1 \leq x \leq 2$, $1 \leq y \leq 2$, $1 \leq z \leq 12$) and constructed ternary Ca-Al-H phase diagrams at 50 and 200 GPa, respectively. As shown in Fig.1, the red solid and hollow circles represent stable and metastable ternary hydrides, respectively. We predicted several stable and metastable ternary hydrides. $Cmcm$ - CaAlH_5 and $Pnmm$ - CaAl_2H_8 are stable at 50 GPa; $P2_1/m$ - CaAlH_5 , and $P4/mmm$ - CaAlH_7 are stable up to 200 GPa; $Immm$ - $\text{Ca}_2\text{AlH}_{12}$ is metastable (31 meV/atom above the convex hull at 200 GPa), and this does not preclude $\text{Ca}_2\text{AlH}_{12}$ from experimental synthesis because many compounds observed in the high-pressure experiments were metastable^[41-43]. The elements and binary hydrides that are stable under high pressures were referred from previous works^[15,39,40,44].

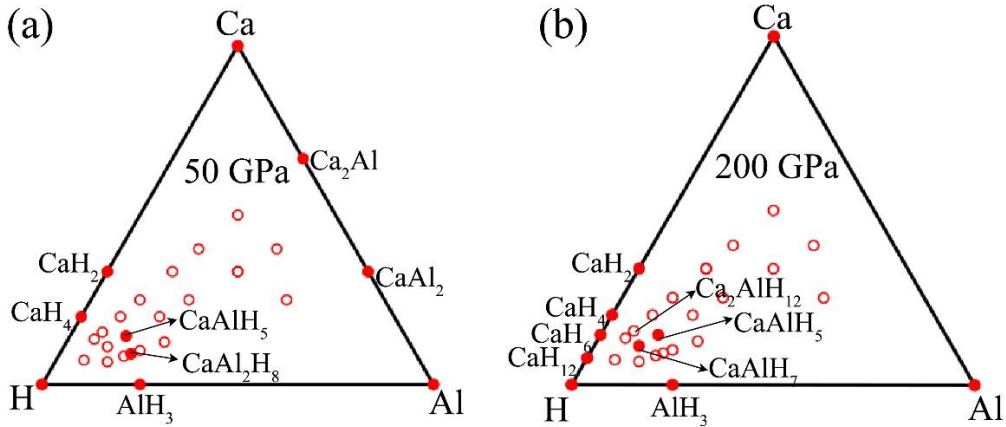


Fig.1. Ternary phase diagrams of the Ca-Al-H system at different pressures. Solid red circles indicate stable structures and open red circles indicate metastable structures.

The crystal structures of the $P4/mmm$ - CaAlH_7 and $Immm$ - $\text{Ca}_2\text{AlH}_{12}$ are shown in Fig. 2, and crystal structure of other hydrides can be found in Supplementary Material Fig. S1, and their detailed lattice parameters and atomic coordinates are shown in the Table S1 of the Supplementary Material. As can be seen from Fig. 2(c), CaAlH_5 is thermodynamic stable above 50 GPa, and it has two energy-competing structures. According to our calculations, at 50-90 GPa and 120-130 GPa, the enthalpy of the $Cmcm$ phase is lower than that of the $P2_1/m$. However, at 90-120 GPa and 130-200 GPa, the enthalpy of the $P2_1/m$ phase is lower than that of the $Cmcm$ phase and

becomes more stable. CaAlH_7 has a thermodynamically stable interval of 80-200 GPa and the phase transform from $Cmcm$ to $P4/mmm$ occurs at 120 GPa.

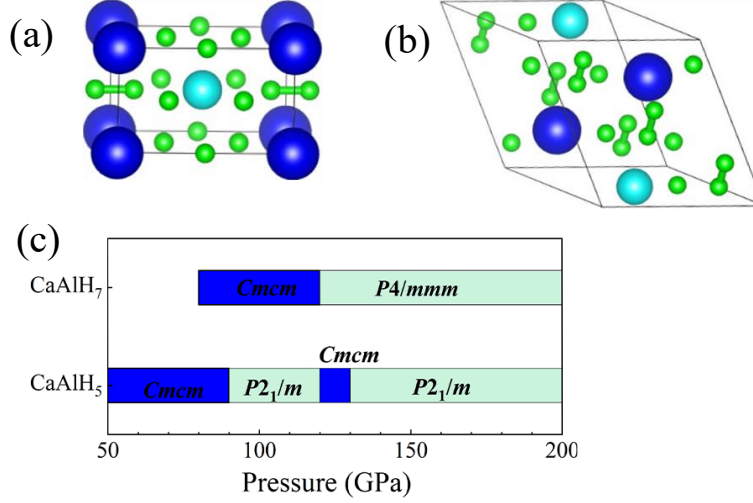


Fig.2. The crystal structures of (a) $P4/mmm$ - CaAlH_7 and (b) $Immm$ - $\text{Ca}_2\text{AlH}_{12}$. Calcium atoms are blue, aluminum atoms are cyan, and hydrogen atoms are green. (c) Predicted pressure-composition phase diagram of CaAlH_5 and CaAlH_7 .

Because there are relatively abundant precursors, ternary Ca-Al-H compounds can be synthesized through different routes under high pressure. For example, $\text{Ca} + \text{Al} + \text{H}_2$, $\text{Ca} + \text{AlH}_3 + \text{H}_2$, $\text{CaH}_2 + \text{Al} + \text{H}_2$, $\text{CaH}_4 + \text{Al} + \text{H}_2$, $\text{CaH}_6 + \text{Al} + \text{H}_2$, $\text{CaH}_2 + \text{AlH}_3 + \text{H}_2$, $\text{CaH}_4 + \text{AlH}_3 + \text{H}_2$. Here we mainly focus on five possible synthetic routes ($\text{Ca} + \text{Al} + \text{H}_2$, $\text{Ca} + \text{AlH}_3 + \text{H}_2$, $\text{CaH}_2 + \text{Al} + \text{H}_2$, $\text{CaH}_2 + \text{AlH}_3 + \text{H}_2$, $\text{CaH}_4 + \text{Al} + \text{H}_2$) and calculate their enthalpies of formation, as shown in Table I. Comparing the formation enthalpies of various synthesis routes, compressing the mixture of $\text{CaH}_2 + \text{AlH}_3 + \text{H}_2$ is the most favorable route to synthesize $\text{Ca}_x\text{Al}_y\text{H}_z$ (see Table I). From another perspective, CaAlH_z ($z > 5$) can also be synthesized by extruding $\text{CaAlH}_5 + \text{H}_2$. We believe that some other synthetic routes may be obtained by extending the precursors or changing the combinations. Once these synthetic pathways are identified, they can provide informative guidance for future experimental synthesis.

TABLE I. Formation enthalpies (eV/atom) of $\text{Ca}_x\text{Al}_y\text{H}_z$ at 50 and 200 GPa. ΔH_1 , ΔH_2 , ΔH_3 , ΔH_4 , ΔH_5 represent the formation enthalpies of $\text{Ca}_x\text{Al}_y\text{H}_z$ from $\text{Ca} + \text{Al} + \text{H}_2$, $\text{Ca} + \text{AlH}_3 + \text{H}_2$, $\text{CaH}_2 + \text{Al} + \text{H}_2$, $\text{CaH}_2 + \text{AlH}_3 + \text{H}_2$, and $\text{CaH}_4 + \text{Al} + \text{H}_2$, respectively.

		ΔH_1	ΔH_2	ΔH_3	ΔH_4	ΔH_5
50 GPa	$Cmcm$ - CaAlH_5	-0.788	-0.676	-0.226	-0.115	-0.178
	$Pnmm$ - CaAl_2H_8	-0.581	-0.438	-0.223	-0.081	-0.190
	$P2_1/m$ - CaAlH_5	-0.847	-0.498	-0.385	-0.036	-0.254
200 GPa	$P4/mmm$ - CaAlH_7	-0.765	-0.493	-0.405	-0.134	-0.303
	$Immm$ - $\text{Ca}_2\text{AlH}_{12}$	-0.724	-0.561	-0.293	-0.130	-0.170

B. Electronic properties of ternary hydrides

Electronic band structures and density of states (DOS) are used to analyze electronic properties. As shown in Fig.3, we found that $Cmcm$ - CaAlH_5 and $Pnmm$ - CaAl_2H_8 are indirect bandgap semiconductors at 50 GPa. $P2_1/m$ - CaAlH_5 exhibit weak metallic states, and the DOS near

the Fermi level is almost zero (see Fig. S2 in the Supplemental Material), so we infer that this structure do not have high temperature superconductivity. The conduction and valence bands of $P4/mmm$ -CaAlH₇ and $Immm$ -Ca₂AlH₁₂ overlap at the Fermi level, and the electronic density of states at the Fermi level is dominated by the electrons from H, as shown in Fig.3, which means that these two structures may have better superconducting properties. Then, we mainly discuss these two structures.

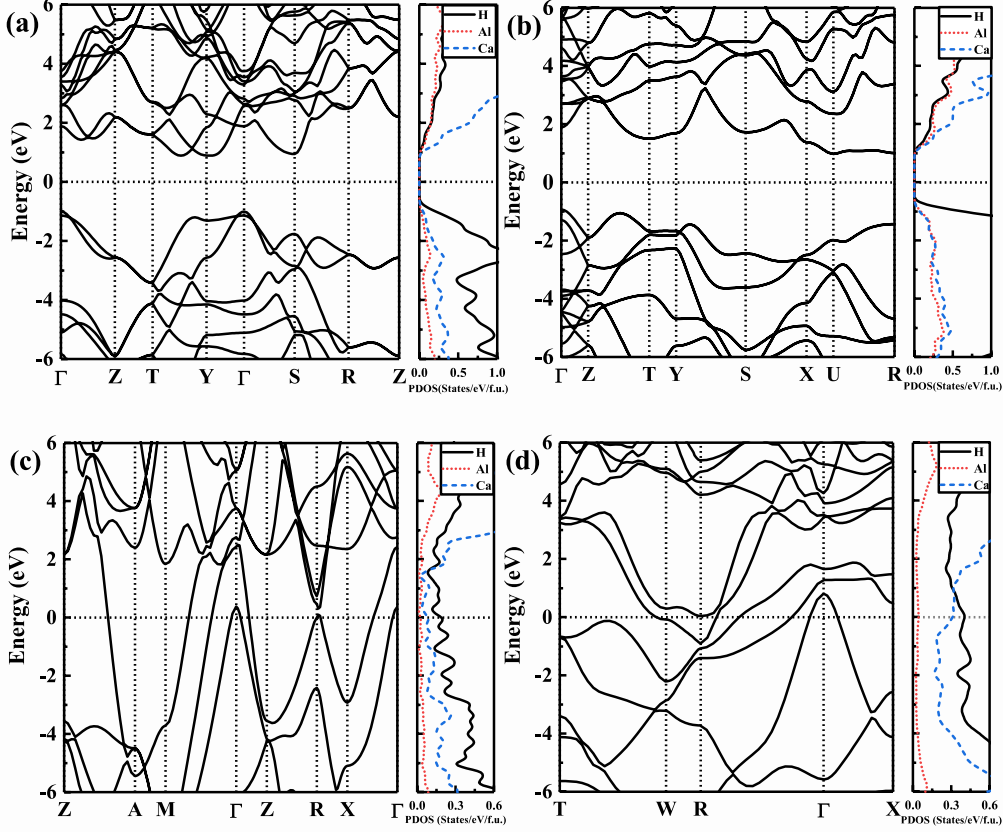


Fig.3. The band structures and partial electronic density of states (PDOS) of (a) $Cmcmm$ -CaAlH₅ at 50 GPa and (b) $Pnnm$ -CaAl₂H₈ at 50 GPa, (c) $P4/mmm$ -CaAlH₇ at 200 GPa, and (d) $Immm$ -Ca₂AlH₁₂ at 250 GPa.

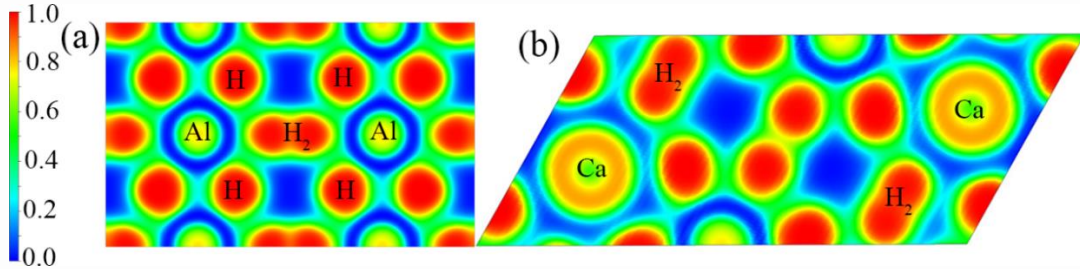


Fig.4. Electronic localization function (ELF) of (a) $P4/mmm$ -CaAlH₇ at 200 GPa and (b) $Immm$ -Ca₂AlH₁₂.

To explore the bonding information of these compounds, we calculated the electron localization function (ELF) of $P4/mmm$ -CaAlH₇ and $Immm$ -Ca₂AlH₁₂, as shown in Fig. 4. For $P4/mmm$ -CaAlH₇ and $Immm$ -Ca₂AlH₁₂, there are no localized electrons between Ca/Al and H, indicating that between Ca/Al and H are pure ionic bonds. The ELF values between the nearest

hydrogen atoms of $P4/mmm$ -CaAlH₇ and $Immm$ -Ca₂AlH₁₂ are 0.93 and 0.95, respectively, indicating that there is a relatively strong covalent bond between the H atoms. Their charge transfer is different, so they correspond to different ELF values. Moreover, the transfer of charge also affects the distance between H molecules.

In order to further understand their bonding information, we calculated the bader charges of CaAlH₇ at 50-200 GPa and Ca₂AlH₁₂ at 250 GPa. The bader charge analysis in Table II shows that the charge is transferred from Ca and Al to H₂ and isolated H atoms. In CaAlH₇, Ca and Al lose charges greater than 1.05 e and 2.42 e , respectively. The gain of each isolated H atom is about 0.48-0.5 e to form H⁻ ions, and within 50-200 GPa, the electron gains of the H₂ unit electrons are 0.52 e , 0.44 e , 0.47 e , 0.5 e , respectively. At 250 GPa, Ca and Al lose charges greater than 0.88 e and 2.39 e in Ca₂AlH₁₂, respectively. Each isolated H atom has a gain of 0.34-0.35 e , forming an H⁻ ion, and the electron gain of the H₂ unit is 0.17 e in Ca₂AlH₁₂. It can be clearly seen that Ca is a better electron donor than Na under corresponding pressure^[26]. Furthermore, the maximum distance between H atoms in the H₂ unit in CaAlH₇ is 0.93 Å, and the distance between H atoms in the H₂ molecule in Ca₂AlH₁₂ is 0.84 Å, which is obviously longer than the H-H bond of free H₂, which is 0.74 Å. It is also longer than the H₂ bond length in the Na-Al-H system. We think this is the transfer of Ca and Al electrons to H₂, and these extra electrons occupy the antibonding orbital of H-H, thus weakening the strength of H-H bond, thereby increasing the distance of H-H. Especially for CaAlH₇, the length of H-H bond increases monotonically with the number of extra electrons within 100-200 GPa. Furthermore, compared with sodium, calcium can provide more electrons to occupy the antibonding orbital of H-H bond, thus weakening the covalent bond between quasi-hydrogen molecules to a greater extent, resulting in the emergence of more quasi-atomic hydrogen, which makes the electrons of hydrogen in the Fermi level of CaAlH₇ more than NaAlH₇ and NaAlH₈^[26]. This means that it is possible to be beneficial to the superconducting properties for the CaAlH₇.

TABLE II. Bader analysis for CaAlH₇ at 50, 100, 150, and 200 GPa, and Ca₂AlH₁₂ at 250 GPa.

$\delta(e)$	50 GPa	100 GPa	150 GPa	200 GPa	250 GPa
	CaAlH ₇				Ca ₂ AlH ₁₂
H	-0.49~-0.5	-0.48~-0.49	-0.49~-0.5	-0.48~-0.49	-0.34~-0.35
H ₂	-0.52	-0.44	-0.47	-0.5	-0.17
Ca	1.05	1.05	1.04	0.99	0.88
Al	2.42	2.37	2.43	2.42	2.39

C. Phonon dispersion and superconductivity properties of ternary hydrides

Phonon dispersion curves, projected phonon density of states (PHDOS), Eliashberg spectral function $\alpha^2F(\omega)$, and electronic phonon integrals $\lambda(\omega)$ for $P4/mmm$ -CaAlH₇ and $Immm$ -Ca₂AlH₁₂ are shown in Fig.5. There are no imaginary frequencies throughout the Brillouin zone for all the ternary hydrides, suggesting the dynamical stability. The minimum pressure for dynamical stable of $P4/mmm$ -CaAlH₇ is 50 GPa, but the minimum pressure for dynamical stability of $Immm$ -Ca₂AlH₁₂ is 250 GPa. For these stable structures, their contributions to the phonon spectrum and PHDOS are also significantly different due to the different atomic masses. The low frequency vibration modes (0-15 THz) are mainly related to Ca and Al atoms, and the high frequency region is mainly related to the H atom vibration modes, as shown in the Fig.5. The peak of the Eliashberg spectral function $\alpha^2F(\omega)$ and the larger rising region of the electron-phonon integral $\lambda(\omega)$ appear in

the high-frequency region associated with the vibrational modes of the H atom, indicating that the hydrogen atoms play a dominant role in the electron-phonon interaction. Importantly, we find that many soft phonon modes emerge in the mid-frequency region of the phonon dispersion curve, as shown in Fig.5. At 200 GPa, $P4/mmm$ -CaAlH₇, along the Z-A direction, and points A and X appear significantly softening of phonon modes. When the pressure is 50 GPa, the softening of these optical branches will be more obvious. The spectral function $\alpha^2F(\omega)$ and EPC integral $\lambda(\omega)$ are also shown in Fig.5. At 50 GPa, it is found that the low-frequency and high-frequency EPC contribute for 39% and 61% of the total EPC, respectively. At 200 GPa, the proportions are 22% and 78%, respectively. In other words, at 50 and 200 GPa, the derivatization frequencies of H contributed 61% and 78% of the total, respectively, which is relatively common in hydrides at high pressure. In addition, the superconducting transition temperatures were calculated by solving the Allen-Dynes modified McMillan equation^[38]:

$$T_c = \frac{\omega_{\log}}{1.2} \exp \left[-\frac{1.04(1+\lambda)}{\lambda - \mu^* (1+0.62\lambda)} \right]$$

Coulomb potential $\mu^*=0.1-0.13$, for $\lambda < 1.5$, this equation can provide high precision T_c value. As shown in Table III, at 50 GPa, the T_c of $P4/mmm$ -CaAlH₇ is 71 K, the electron-phonon coupling coefficient λ is 1.28, the logarithmic average phonon frequency ω_{\log} is 658 K. With the pressure increases, the phonons tend to exhibit hardening, the ω_{\log} slowly increases, and the EPC parameter λ decreases significantly, so the T_c of CaAlH₇ decreases significantly.

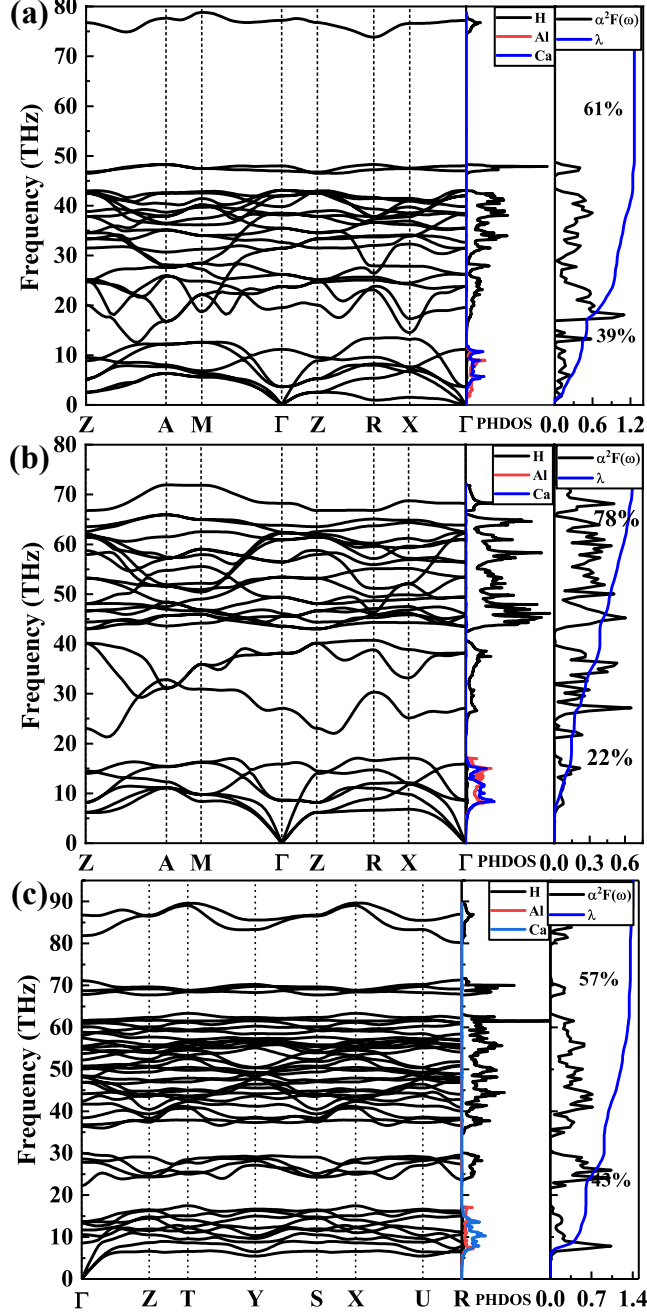


Fig.5. Calculated phonon dispersion curves, projected phonon density of states (PHDOS), and Eliashberg spectral function $\alpha^2 F(\omega)$ together with the electron-phonon integral $\lambda(\omega)$ for (a) $P4/mmm$ - CaAlH_7 at 50 GPa, (b) $P4/mmm$ - CaAlH_7 at 200 GPa, (c) $Immm$ - $\text{Ca}_2\text{AlH}_{12}$ at 250 GPa.

TABLE III. The calculated EPC parameter λ , logarithmic average phonon frequency ω_{log} (K), electronic density of states at Fermi level $N(\epsilon_f)$ (states/spin/Ry/f.u.), and superconducting transition temperatures T_c (K) with $\mu^*=0.1-0.13$ at corresponding pressures P (GPa).

Structure	P (GPa)	λ	ω_{log} (K)	$N(\epsilon_f)$ (states/spin/Ry/f.u.)	T_c (K)
$P4/mmm$ - CaAlH_7	50	1.28	658	3.9	62-71
	100	0.82	1166	3.2	49-61
	150	0.72	1367	2.9	41-53
	200	0.66	1498	2.8	35-47
$Immm$ - $\text{Ca}_2\text{AlH}_{12}$	250	1.4	979	6.8	105-118

IV. CONCLUSIONS

In summary, we comprehensively investigated the structural phase diagram, electronic properties, lattice dynamics and superconductivity of the Ca-Al-H ternary system under pressure. We found stable $P4/mmm$ -CaAlH₇ and metastable $Immm$ -Ca₂AlH₁₂ under high pressure, the superconducting transition temperature of CaAlH₇ can reach 71 K at 50 GPa, and the superconducting transition temperature of Ca₂AlH₁₂ can reach 118 K at 250 GPa. The phonon softening along the Z-A direction and at point X have positive contribution to superconductivity of CaAlH₇. In addition, we proposed several possible synthetic routes for Ca-Al-H compounds, which will contribute to subsequent experimental studies. These results also provide an important reference for the exploration of other superconducting hydrides.

- [1] J. Bardeen, L. N. Cooper and J. R. Schrieffer, *Physical Review* **108**, 1175 (1957).
- [2] N. W. Ashcroft, *Phys. Rev. Lett.* **21**, 1748 (1968).
- [3] M. I. Eremets, A. P. Drozdov, P. P. Kong and H. Wang, *Nature Physics* **15**, 1246 (2019).
- [4] V. L. Ginzburg, *Journal of Statistical Physics* (1969).
- [5] Y. Li, J. Hao, H. Liu, Y. Li and Y. Ma, *J Chem Phys* **140**, 174712 (2014).
- [6] N. W. Ashcroft, *Phys Rev Lett* **92**, 187002 (2004).
- [7] D. Duan, Y. Liu, Y. Ma, Z. Shao, B. Liu and T. Cui, *National Science Review* **4**, 121 (2017).
- [8] D. Duan, H. Yu, H. Xie and T. Cui, *Journal of Superconductivity and Novel Magnetism* **32**, 53 (2018).
- [9] J. A. Flores-Livas, L. Boeri, A. Sanna, G. Profeta, R. Arita and M. Eremets, *Physics Reports* **856**, 1 (2020).
- [10] D. V. Semenok, I. A. Kruglov, I. A. Savkin, A. G. Kvashnin and A. R. Oganov, *Current Opinion in Solid State and Materials Science* **24** (2020).
- [11] H. Xie, Y. Yao, X. Feng, D. Duan, H. Song, Z. Zhang, S. Jiang, S. A. T. Redfern, V. Z. Kresin, C. J. Pickard and T. Cui, *Phys Rev Lett* **125**, 217001 (2020).
- [12] D. Duan, F. Tian, X. Huang, D. Li, H. Yu, Y. Liu, Y. Ma, B. Liu and T. Cui, *arXiv:1504.01196* (2015).
- [13] F. Peng, Y. Sun, C. J. Pickard, R. J. Needs, Q. Wu and Y. Ma, *Phys Rev Lett* **119**, 107001 (2017).
- [14] A. G. Kvashnin, D. V. Semenok, I. A. Kruglov, I. A. Wrona and A. R. Oganov, *ACS Appl Mater Interfaces* **10**, 43809 (2018).
- [15] H. Wang, J. S. Tse, K. Tanaka, T. Iitaka and Y. Ma, *Proc Natl Acad Sci U S A* **109**, 6463 (2012).
- [16] A. P. Drozdov, P. P. Kong, V. S. Minkov, S. P. Besedin, M. A. Kuzovnikov, S. Mozaffari, L. Balicas, F. F. Balakirev, D. E. Graf, V. B. Prakapenka, E. Greenberg, D. A. Knyazev, M. Tkacz and M. I. Eremets, *Nature* **569**, 528 (2019).
- [17] I. Errea, F. Belli, L. Monacelli, A. Sanna, T. Koretsune, T. Tadano, R. Bianco, M. Calandra, R. Arita, F. Mauri and J. A. Flores-Livas, *Nature* **578**, 66 (2020).
- [18] H. Liu, Naumov, II, R. Hoffmann, N. W. Ashcroft and R. J. Hemley, *Proc Natl Acad Sci U S A* **114**, 6990 (2017).
- [19] M. Somayazulu, M. Ahart, A. K. Mishra, Z. M. Geballe, M. Baldini, Y. Meng, V. V. Struzhkin and R. J. Hemley, *Physical Review Letters* **122** (2019).
- [20] A. P. Drozdov, M. I. Eremets, I. A. Troyan, V. Ksenofontov and S. I. Shylin, *Nature* **525**, 73 (2015).
- [21] D. Duan, X. Huang, F. Tian, D. Li, H. Yu, Y. Liu, Y. Ma, B. Liu and T. Cui, *Physical Review B* **91**

- (2015).
- [22] D. Duan, Y. Liu, F. Tian, D. Li, X. Huang, Z. Zhao, H. Yu, B. Liu, W. Tian and T. Cui, *Sci Rep* **4**, 6968 (2014).
- [23] M. Einaga, M. Sakata, T. Ishikawa, K. Shimizu, M. I. Eremets, A. P. Drozdov, I. A. Troyan, N. Hirao and Y. Ohishi, *Nat Phys* **12**, 835 (2016).
- [24] S. Di Cataldo, W. von der Linden and L. Boeri, *Physical Review B* **102** (2020).
- [25] H. Li, T. Gao, S. Ma and X. Ye, *Phys Chem Chem Phys* **24**, 8432 (2022).
- [26] H. Song, Z. Zhang, M. Du, Q. Jiang, D. Duan and T. Cui, *Physical Review B* **104** (2021).
- [27] Y. Sun, J. Lv, Y. Xie, H. Liu and Y. Ma, *Phys Rev Lett* **123**, 097001 (2019).
- [28] W.-H. Yang, W.-C. Lu, W. Qin, H.-J. Sun, X.-Y. Xue, K. M. Ho and C. Z. Wang, *Physical Review B* **104** (2021).
- [29] C. J. Pickard and R. J. Needs, *Phys. Rev. Lett.* **97**, 045504 (2006).
- [30] C. J. Pickard and R. J. Needs, *J Phys Condens Matter* **23**, 053201 (2011).
- [31] M D Segall¹, Philip J D Lindan^{3,7},MJProbert⁴, C J Pickard¹,PJ Hasnip⁵, S J Clark⁶ andMCPayne¹, *J. Phys.: Condens. Matter* **14** 2717 (2002).
- [32] M. C. Payne, M. P. Teter, D. C. Allan, T. A. Arias and J. D. Joannopoulos, *Reviews of Modern Physics* **64**, 1045 (1992).
- [33] I. Stewart J. Clark*, Matthew D. Segall^{III}, Chris J. Pickard^{II}, Phil J. Hasnip^{III}, Matt I. J. Probert^{IV}, Keith Refson^V and Mike C. Payne^{II}, *Z. Kristallogr.* (2004).
- [34] G. K. a. J. Furthmüller, *Computational Materials Science* (1996).
- [35] G. Kresse, *PHYSICAL REVIEW B* (1998).
- [36] K. B. John P. Perdew, * Matthias Ernzerhof, (1996).
- [37] P. Giannozzi, S. Baroni, N. Bonini, M. Calandra, R. Car, C. Cavazzoni, D. Ceresoli, G. L. Chiarotti, M. Cococcioni, I. Dabo, A. Dal Corso, S. de Gironcoli, S. Fabris, G. Fratesi, R. Gebauer, U. Gerstmann, C. Gougoussis, A. Kokalj, M. Lazzeri, L. Martin-Samos, N. Marzari, F. Mauri, R. Mazzarello, S. Paolini, A. Pasquarello, L. Paulatto, C. Sbraccia, S. Scandolo, G. Sclauzero, A. P. Seitsonen, A. Smogunov, P. Umari and R. M. Wentzcovitch, *J Phys Condens Matter* **21**, 395502 (2009).
- [38] P. B. Allen and R. C. Dynes, *Phys. Rev. B* **12**, 905 (1975).
- [39] K. Abe, *Physical Review B* **100** (2019).
- [40] Z. Shao, D. Duan, Y. Ma, H. Yu, H. Song, H. Xie, D. Li, F. Tian, B. Liu and T. Cui, *Inorg Chem* **58**, 2558 (2019).
- [41] Z. D. D. Campanini, and A. Rydh, *Physical Review B* **97** (2018).
- [42] M. G. i. John S. C. Kearney, Dean Smith,* Daniel Sneed, Christian Childs, Jasmine Hinton, Changyong Park, Jesse S. Smith, Eunja Kim, Samuel D. S. Fitch, Andrew L. Hector,Chris J. Pickard, JosØ A. Flores-Livas,* and Ashkan Salamat*, *Angew Chem Int Ed Engl* **57**, 11623 (2018).
- [43] A. S. José A. Flores-Livas, 2Alexander P. Drozdov, Lilia Boeri,Gianni Profeta,Mikhail Eremets,and Stefan Goedecker, *Physical Review Materials* **1** (2017).
- [44] C. J. Pickard and R. J. Needs, *Nature Physics* **3**, 473 (2007).

Supplementary information for

“Phase diagrams and superconductivity of ternary Ca-Al-H compounds under high pressure”

Ming Xu¹, Defang Duan², Wendi Zhao¹, Decheng An² Hao Song^{1,*} and Tian Cui^{1,2†}

¹Institute of High Pressure Physics, School of Physical Science and Technology, Ningbo University, Ningbo 315211, China

²State Key Laboratory of Superhard Materials, College of Physics, Jilin University, Changchun 130012, China

*Corresponding author: songhao@nbu.edu.cn

†Corresponding author: cuitian@nbu.edu.cn

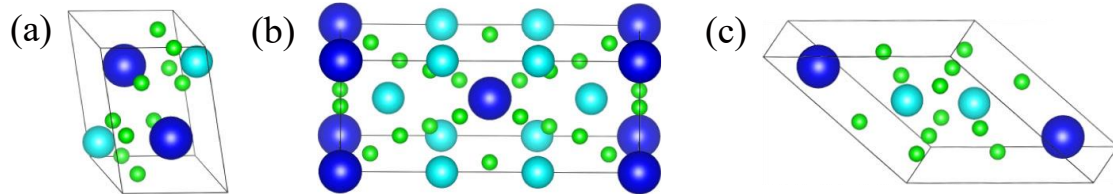


Fig. S1. The crystal structures of (a) $Cmcm$ - $CaAlH_5$ (b) $Pnnm$ - $CaAl_2H_8$ (c) $P2_1/m$ - $CaAlH_5$. Among them, calcium atoms are dark blue, aluminum atoms are light blue, and hydrogen atoms are green.

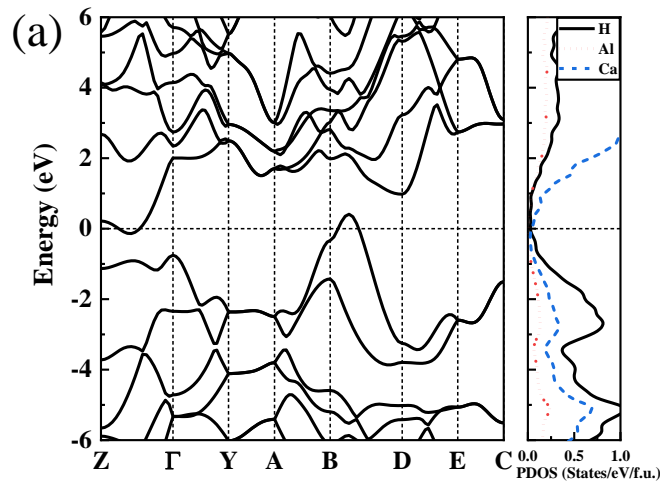


Fig. S2. The band structures and partial electronic density of states (PDOS) of $P2_1/m$ - $CaAlH_5$ at 200 GPa using the GGA-PBE functionals.

Table S1. Structural information of predicted hydrides.

Structure	Lattice parameters(Å)		Atomic coordinates			Sites
<i>P4/mmm</i> CaAlH ₇ 200 GPa	a=b=2.6015 c=4.2674 $\alpha=\beta=\gamma=90^\circ$	H1	0.000000	1.000000	-0.889920	2g
		H2	0.000000	0.500000	-0.288020	4i
		H3	0.500000	0.500000	-0.500000	1d
		Al	0.000000	0.000000	-0.500000	1b
		Ca	-0.500000	0.500000	0.000000	1c
<i>P2₁/m</i> CaAlH ₅ 200 GPa	a= 5.0112 b= 3.7364 c= 3.2078 $\alpha=\gamma=90^\circ$ $\beta= 63.9052^\circ$	H1	0.495540	0.496650	0.206350	4f
		H2	-0.115550	0.454200	0.244450	4f
		H3	0.194180	0.250000	1.210440	2e
		Al	0.662960	0.750000	0.377780	2e
		Ca	0.186540	0.750000	0.209030	2e
<i>Cmcm</i> CaAlH ₅ 50 GPa	a= 3.8830 b= 3.4174 c= 8.8034 $\alpha=\beta=\gamma=90^\circ$	H1	-0.114290	0.211810	0.800710	8h
		H2	0.748210	-0.505780	0.500000	4g
		H3	1.000000	0.000000	0.601300	4e
		Al	0.500000	0.000000	0.839420	4f
		Ca	0.000000	-0.500000	1.000000	4c
Ca ₂ AlH ₁₂ <i>Immm</i> 200 GPa	a= 8.0124 b= 4.4908 c= 2.6524 $\alpha=\beta=\gamma=90^\circ$	H1	0.000000	-0.398440	-1.500000	4h
		H2	0.343450	-0.716860	-1.000000	8n
		H3	0.186400	-0.908070	-1.000000	8n
		H4	0.000000	-0.805120	-2.000000	4g
		Al	0.000000	0.000000	-0.500000	2c
		Ca	0.342920	1.000000	-1.500000	4f
CaAl ₂ H ₈ <i>Pnnm</i> 50 GPa	a= 3.8830 b= 3.4174 c= 8.8034 $\alpha=\beta=\gamma=90^\circ$	H1	-0.114290	0.211810	0.800710	8h
		H2	0.748210	-0.505780	0.500000	4g
		H3	1.000000	0.000000	0.601300	4e
		Al	0.500000	0.000000	0.839420	4f
		Ca	0.000000	-0.500000	1.000000	4c